

We are IntechOpen, the world's leading publisher of Open Access books Built by scientists, for scientists

6,500

Open access books available

176,000

International authors and editors

190M

Downloads

Our authors are among the

154

Countries delivered to

TOP 1%

most cited scientists

12.2%

Contributors from top 500 universities



WEB OF SCIENCE™

Selection of our books indexed in the Book Citation Index
in Web of Science™ Core Collection (BKCI)

Interested in publishing with us?
Contact book.department@intechopen.com

Numbers displayed above are based on latest data collected.
For more information visit www.intechopen.com



Chapter

Landslide Assessment and Hazard Zonation in the Birbir Mariam District, Gamo Highlands, Rift Valley Escarpment, Ethiopia

Yonas Oyda and Hailu Regasa

Abstract

The current research focused on landslide assessment and hazard zonation in the Birbir Mariam district of the Gamo highlands. The study examined landslide causative factors and used the slope susceptibility evaluation parameter to create a landslide hazard zonation covering an area of 110 km². The landslide hazard zonation was classified using facet-wise observation. As a result, the intrinsic and external causal parameters of score schemes have been held responsible for slope instability. Inherent causative elements consist of slope geometry, slope material (rock/soil), structural discontinuities, land use/land cover, and groundwater conditions. Rainfall and human interest have seemed as external elements. The intrinsic and external triggering elements for every facet (a total of 106) were rated for their contribution to slope instability. Finally, an evaluated landslide hazard value was calculated and classified into three landslide hazard classes. According to the findings, the area has a high hazard zone of 18.87% (20.76 km²), a moderate hazard zone of 54.72% (60.19 km²), and a low hazard zone of 26.41% (29.05 km²).

Keywords: Ethiopia, landslide, hazard zonation, landslide evaluation, slope stability

1. Introduction

Landslides are a series of events in which a mass of rocks, soil, or debris slides down a slope due to gravitational pull, the mechanisms include sliding, falling, or flowing material down a slope [1–3]. Landslides are one of the most common geological hazards in the world, with a high incidence, a wide range of distribution, and catastrophic severity, resulting in numerous fatalities each year [3–9].

Landslides are caused by inherent causative parameters such as slope geometry, slope material, structural discontinuities, land use, land cover, and groundwater conditions, which define the unfavorable stability conditions within the slope [4, 10, 11]. External causative factors, such as rainfall, volcanism, seismic motion, and human activities, are also relatively variable or dynamic, temporary, and forced by upcoming

events [11–14], the slope will be prone to instability when the slope morphometry is steep, and a chance of landslide increases with an increase in slope steepness through landslide occurs in all slope. Landslides such as rock-fall, toppling, and rockslides/avalanches are common in the area because the slope material has been covered by highly fractured bedrock such as basalt and ignimbrite [15–17].

Discontinuities in the slope, such as bedding, joints, and faults, are potentially weak planes that affect slope stability [9, 15, 18]. As a result, fractured rocks have lower strength than intact rocks. They are the most vulnerable component of slope geology, and knowledge of their orientation, spacing, continuity, roughness, separation, and type of filling material, as well as slope angle, slope direction, and strength along such potential weak planes, is essential. Slope stability is influenced by land use/land cover, and the material's shear strength is reduced by subsoil conditions in the slope [17, 19, 20].

Landslides are one of Ethiopia's most common natural disasters, and the current study area of the Birbir Miriam district is one of the most vulnerable. A variety of factors affect slope stability, including slope angle, lithology, soil type, and hydrologic conditions [21]. Deforestation, changes caused by the construction of engineering structures on the slope, road construction undercutting the toe of the slope, and other human activities all contribute to potential factors. Variations in human activity on the cliff-side can make the slope less stable [4, 22–25]. Landslides harm infrastructure (houses, roads, buildings, irrigation, canals, and so on), as well as cause geomorphological damage, serious injuries, and the death of humans and animals. For minimizing damage to infrastructure, homes, cultivated lands, and human lives, well-organized landslide hazard zonation is critical. These slope failures zonation maps become significant when they are used by decision-makers in land use planning, landslide prevention, and mitigation methods [8, 15, 26–30].

The goal of a landslide study is to determine the essence of predisposition as well as the outcomes for human life, land, roads, buildings, and other resources [4, 31]. As a result, locating landslide-prone areas is critical for ensuring human safety and avoiding negative consequences for regional and national economies [1, 9, 32–36].

Landslides are common in the Birbir Mariam district along riverbanks, slope toes, and slope faces. Landslides are responsible for any losses and also affect much of the farmland and farmers' income. Moreover, landslides in the study area cause significant damage to properties and massive destruction, particularly in Zala Gutisha and Waro localities, among the heights-prone areas.

2. Materials and methods

2.1 Study area

The current study area is in the Birbir Mariam district of Ethiopia's Gamo highlands, in the rift valley escarpments. It is approximately 450 km from Addis Ababa's capital city and 47 km from the Zonal capital of Arba Minch town. It has a total area of 110 km² and is geographically bounded (UTM Zone 37 N) by latitudes ranging from 692,000 to 702,000 m N and longitudes ranging from 342,000 to 360,000 m E. The area can be reached from Arba Minch town via the Chenchä-Ezo main road and the Birbir Mariam gravel road (**Figure 1**).

The study area's geological setting has a significant impact on the occurrence of landslides. Since the Oligocene, volcanoes have been active in the southern part of the

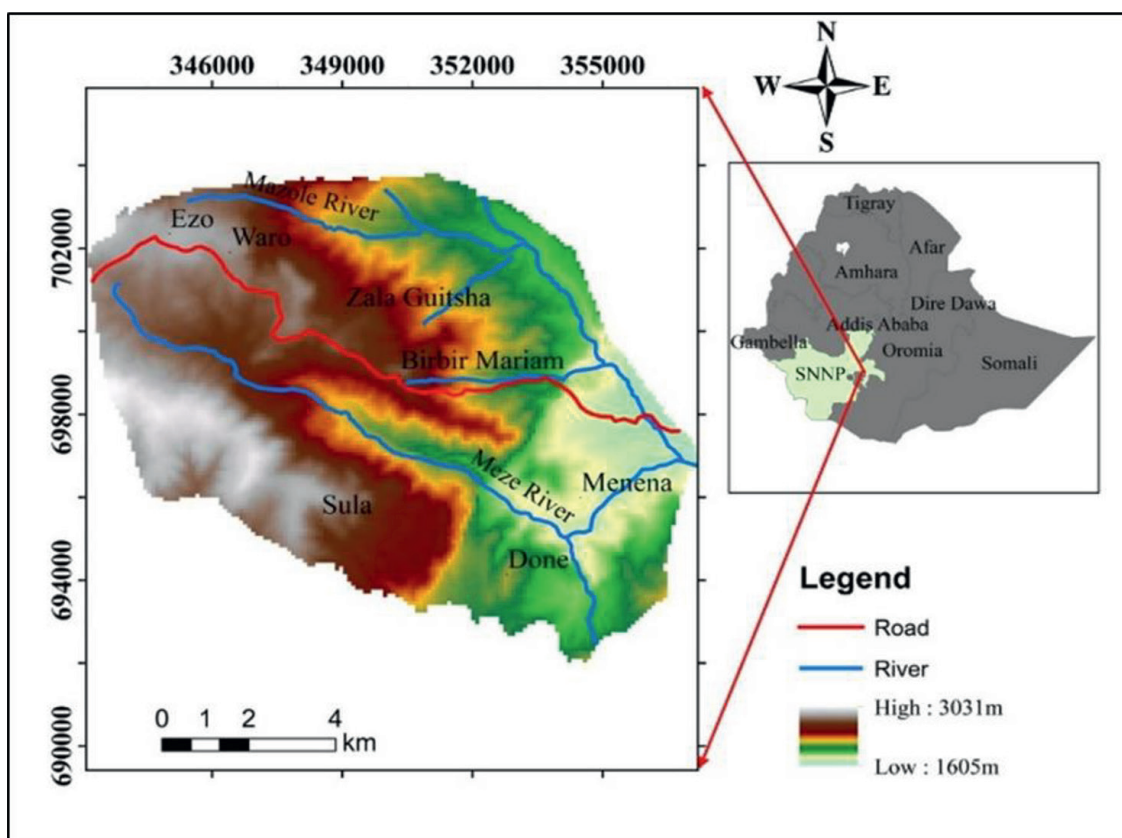


Figure 1.
Location map of Birbir Mariam district.

Main Ethiopian Rift (MER), which includes the Ganjuli graben (Lake Abaya), and the western side of Lake Abaya, which includes the plateau and the Chencha escarpment [37–39]. The geology of the study area is dominated by pre-rift and post-rift deposits. Thereby, the stratigraphy [38, 40] has the following significant units in the Galena basin and north Abaya basin. These are ignimbrite, unwelded tuff units, early flood basalts, alkaline basalt intermediate flows, pyroclastic rocks, Pleistocene basalt, trachyte, and rhyolites.

The geology of the research area can be mapped using field investigations. Basalt, tuff, and Ignimbrite are among the geologic units found in the study area (rock units). The measurement's rock units can be present along rivers, road cuts, and natural hillsides. Overall, the dominance of destructive materials, basalt, and ignimbrite is a crucial feature of the lithologies of this region (**Figure 2**).

2.2 Materials

The Ethiopia Mapping Agency's toposheet number (0637 D1) at a scale of 1:50,000 was used in the current study to demarcate the study area, and a land facet map was created using the topographic map. The slope morphometry and relative relief map were extracted using a DEM (digital elevation model) with a spatial resolution of 12.5 m from the Alaska Satellite Facility site. On January 10, 2019, cloud-free optical satellite data acquired by Landsat-8 Operational Land Imager (OLI) with path-row numbers 170-051 was also entered into the following portal (<http://earth-explorer.usgs.gov/>) and used to develop land use and land cover map of the current study area (**Figure 3**).

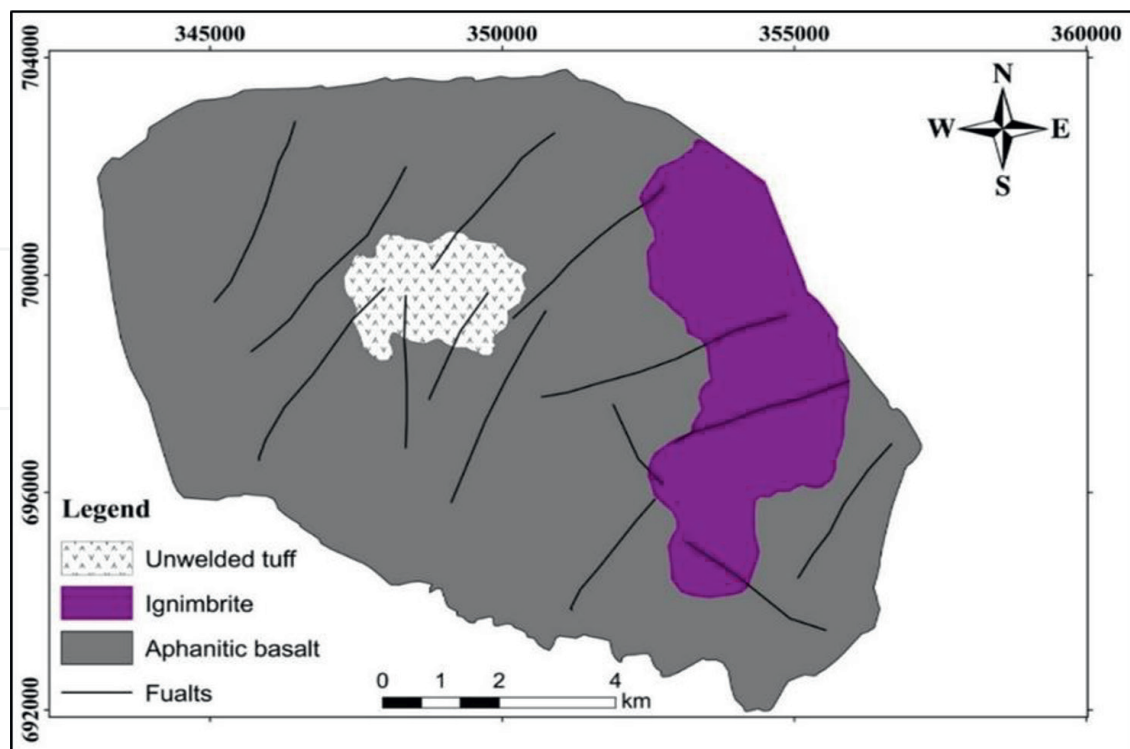


Figure 2.
Geological map of the study area.

2.3 Methods

The entire research area was initially divided into 106 slope land facets (**Figure 4**). In terms of slope inclination and slope direction, a land facet is defined as a land unit with more or less uniform slope geometry [4]. The slope facets were delineated using topographical maps. Facets were defined by major and minor hill ridges, primary and secondary streams, and other topographical undulations [4, 11]. The prepared facet map was then used as a base map for collecting data on the various causative factors. Lithology, structural discontinuity with slope, slope morphometry, relative relief, land use/land cover, groundwater-surface drops, rain-induced index, and human activities are among the factors that contribute to slope instability [4, 11, 12, 41]. As a result, the susceptibility evaluation parameter rating was assigned for each causative factor to get evaluated landslide hazard.

The total maximum susceptibility evaluation parameter rating for the various causative factors is 15. The maximum value was accounted for slope morphometry, groundwater situation, and seismicity 2.0. Land use land cover, rainfall-induced surface index, and human activity contributed to a maximum susceptibility evaluation parameter rate of 1.5. Furthermore, relative relief and slope geo-material each contribute at a rate of 1.0. Structured discontinuity, on the other hand, contributes a maximum susceptibility evaluation parameter rate of 2.50 (**Table 1**). The evaluated landslide hazard is the total sum of susceptibility evaluation parameter ratings for all causative factors; therefore, the greater the value of the susceptibility evaluation parameter, the greater the degree of hazard.

The slope susceptibility evaluation parameter was developed by [11] by taking intrinsic (inherent) and external landslide causative factors. Furthermore, the total prospect of instability was established by assessing landslide hazard, and it was determined facet-by-facet for which observations and investigations were made during

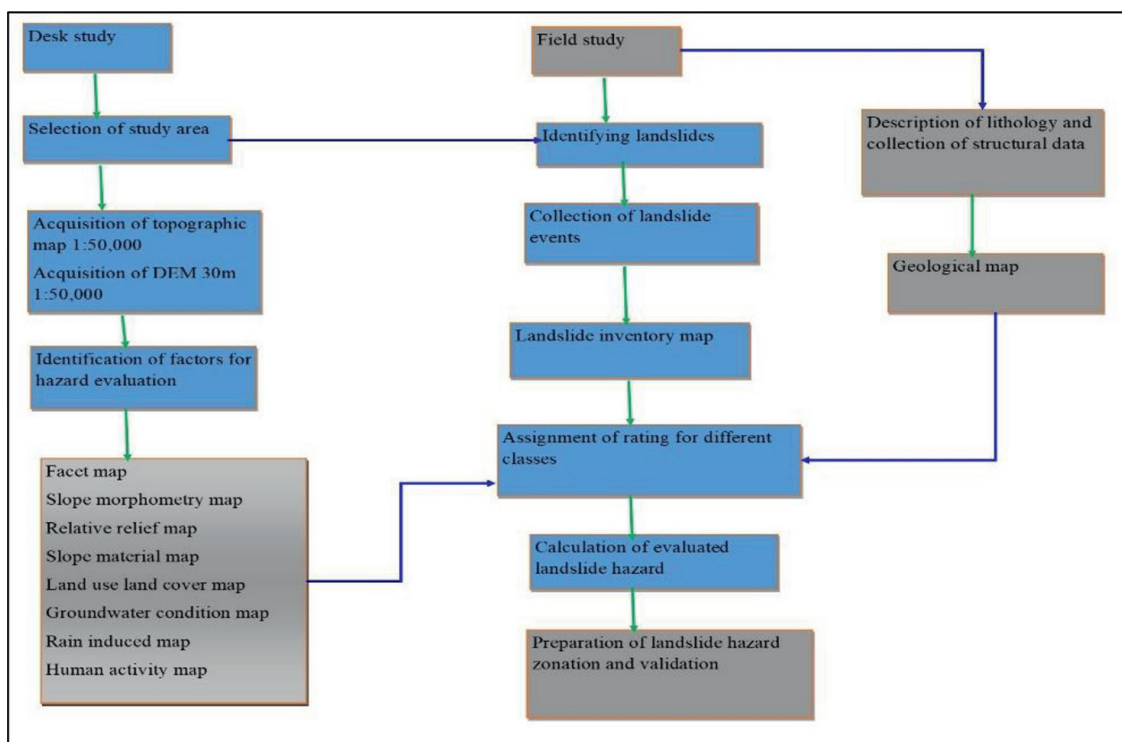


Figure 3.
 General methodology flow chart for the study.

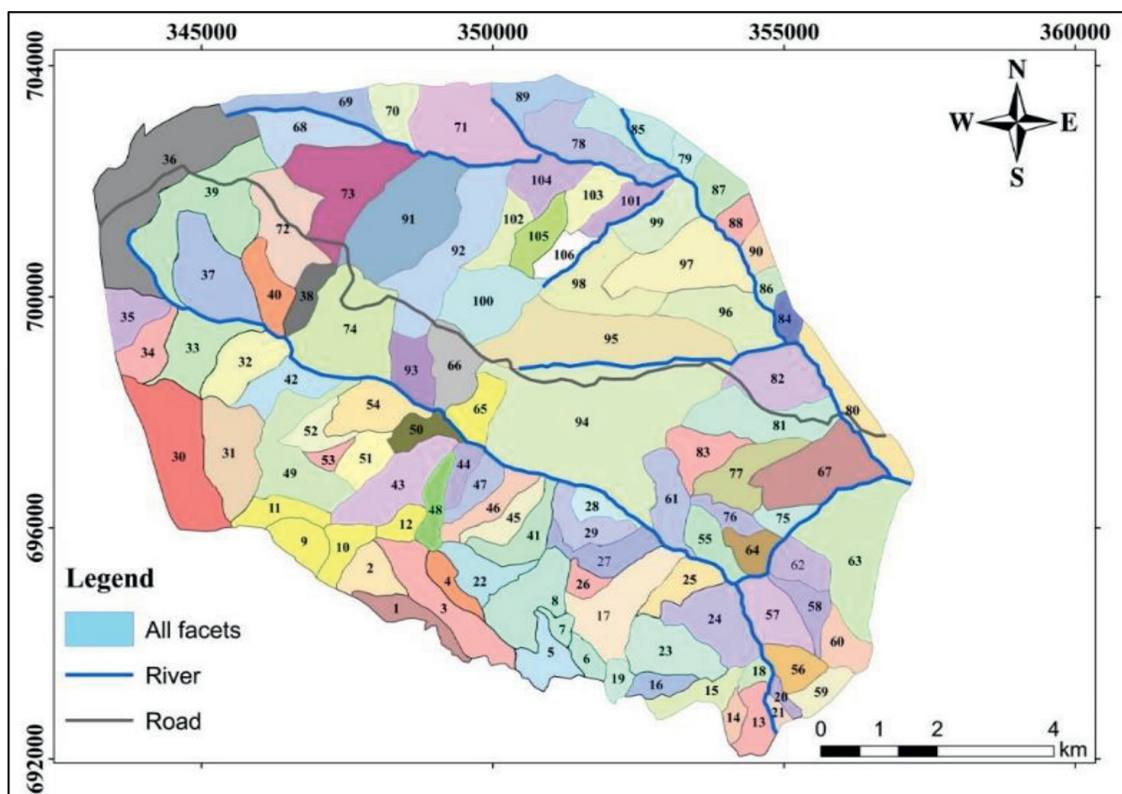


Figure 4.
 Land facet map of the study area.

the fieldwork. As a result, ratings from **Table 1** have been assigned and evaluated landslide hazard is the total sum of susceptibility evaluation parameter ratings for the various causative factors for each facet. Each causative factor was assigned a rate

Code	Susceptibility evaluation parameter (SEP) parameters		Maximum rate assigned (R)	Landslide hazard zone	Landslide hazard class	Evaluated landslide hazard
	Intrinsic parameters			High hazard zone	IV	12-8
R1	Slope geometry	Relative relief	1.0	Moderate hazard zone	III	7.9-5
R2		Slope morphometry	2.0	Low hazard zone	II	4.9-2
R3	Slope geo-material		1.0	Very low hazard zone	I	<2
R4	Structural discontinuity		2.5			
R5	Land use land cover		1.5			
R6	Groundwater condition		2.0			
	External parameters					
R7	Seismicity		2.0			
R8	Rainfall		1.5			
R9	Man-made activity		1.5			
	Total parameters		15.00			

Table 1. Rating methods for both intrinsic, external causative factors and evaluated landslide hazard.

based on subjective decisions attained from past research on intrinsic and external causing factors and their relative contribution to slope instability. Field and literature review data on intrinsic and extrinsic causative factors were incorporated. Finally, each causative parameter was rated on a facet-by-facet basis (**Figure 4**).

3. Results and discussion

3.1 Landslide inventory

Landslide inventory is the base for landslide hazard zonation mapping [5, 28, 33, 35, 42]. A clear understanding of landslide conditions and a more detailed assessment of the landslide hazard of the area concerned are essential to make a systematic landslide inventory. The landslide inventory map depicts the location and characteristics of prior landslides. The geologic, topographic, and climatic conditions that are overcome at the site give an important indication regarding the causes and triggering mechanisms of the past slope failures. Hence, landslide inventory mapping provides helpful insight regarding the potential for future landslide occurrences. Based on relevant literature, historical sources, and classical field survey and mapping, landslide inventory on sliding processes was compiled. The inventory includes 46 different types of mass movements from the past and present that are dispersed throughout the area. The landslide inventories (**Figure 5a**) were collected through the direct field survey method. The density of landslides is very high in the central part of the area which is covered by highly weathered basalt.

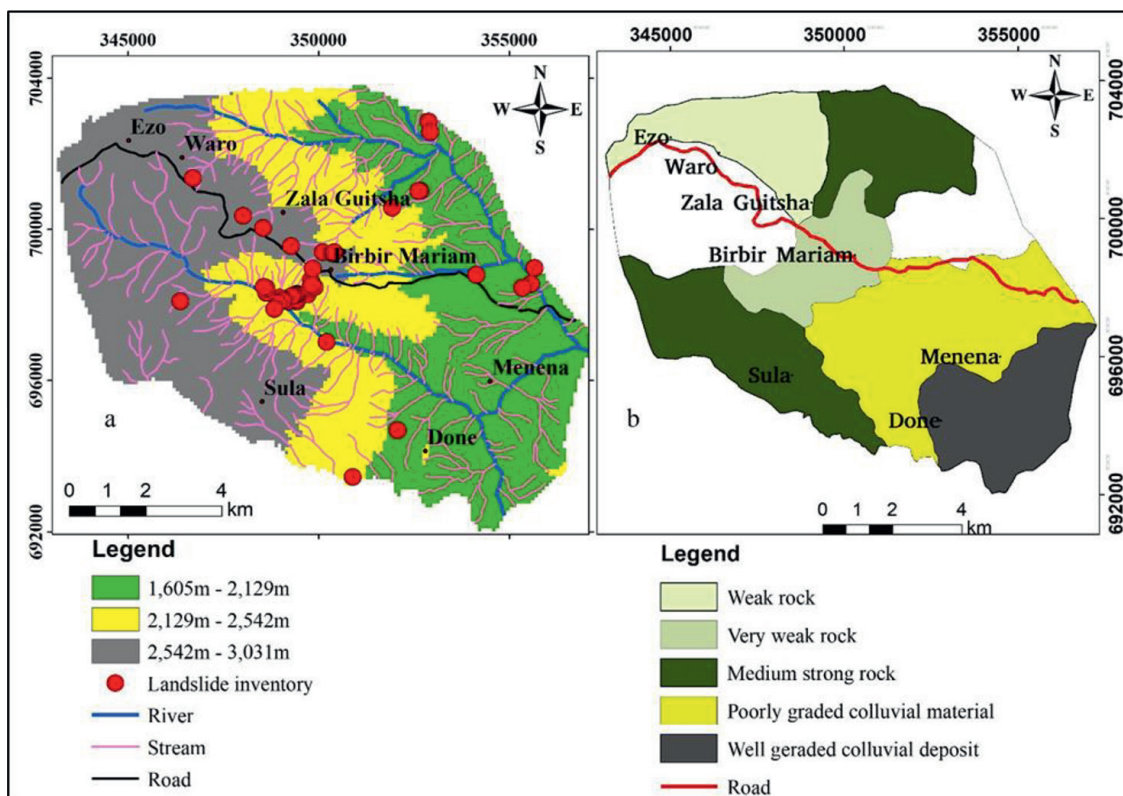


Figure 5.
a. Landslide inventory map of Birbir Mariam district, b. slope geo-material map of Birbir Mariam district.

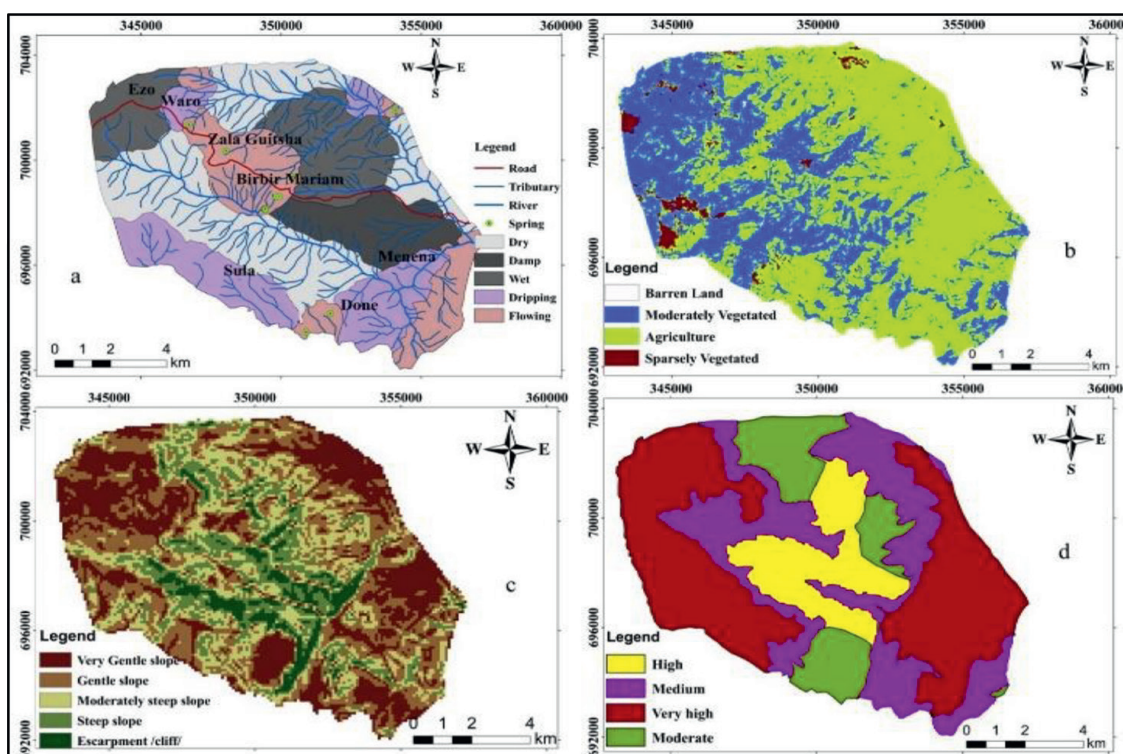


Figure 6.
Landslide causative factor maps, a. groundwater condition manifestation, b. land use land cover, c. slope morphometry, and d. relative relief.

3.2 Landslide causative factors

Intrinsic factors are the inherent or static causative parameters that define the favorable or unfavorable stability conditions within the slope [4, 11]. The main landslide causative factors selected for the Birbir Mariam area are summarized in **Table 1** and their brief descriptions are presented hereunder.

3.2.1 Groundwater condition

Groundwater has a major influence on slope stability. In hilly terrains, groundwater does not follow a consistent pattern and is generally channeled along rock structural discontinuities. It is difficult and time-consuming to assess the behavior of groundwater in hilly terrains over large areas. Groundwater surface indicators (**Figure 6a**) such as damp, wet, dripping, and flowing provide valuable information on the stability of hill slopes and are helpful for the rating [4].

3.2.2 Land use and land cover

Landslides are caused by a variety of factors, including land use and land cover [25]. Thereby, vegetation covers play an important role in slope stabilization through a different mechanism. The land use land cover of the study area (**Figure 6b**) is characterized by agricultural land, bare land, sparsely vegetated land, and moderately vegetated land categories.

3.2.3 Slope morphometry

Slope morphometry is the steepness of the slope [4]. Slope morphology brings to bear major controls on landslide types and the severity of associated damages to life and property. It is classified into five classes (**Figure 6c**) such as escarpment/cliff ($>45^\circ$), steep slope ($36\text{--}45^\circ$), moderately steep slope ($26\text{--}35^\circ$), gentle slope ($16\text{--}25^\circ$), and very gentle slope ($<15^\circ$ [11]).

3.2.4 Relative relief

The difference between a facet's maximum and minimum elevation is known as relative relief. Inside the apiece facet, the relative relief map depicts the local relief of maximum height between the ridge top and valley floor (**Figure 6d**). This relative relief lies on very high, high, medium, and moderate classes in the area based on the slope geometry classification system, and very high-class value range from elevation greater than 300 m, high 201–300 m, medium 101–200 m, and moderate has an elevation of 51–100 m. Therefore, an area with high relative relief is more susceptible to slope failures compared with low relative relief [15, 34, 35].

3.2.5 Lithology

Types of lithologies are the main influencing factors that contributed to the occurrences of landslides in the study area. The dominant lithological units are highly weathered basalts, ignimbrite, tuff, colluvium, alluvial soil deposits, and residual soils overlying the bedrocks (**Figure 5b**). The main criterion in the allocation of the rating for lithological subclasses is the response of the rocks to the weathering processes and erosion. The degree of weathering may vary based on the rock types

and mineralogical compositions. Basalt and ignimbrites form steep slopes because they are hard, massive, and resistant to erosion. Soft rocks, on the other hand, such as tuff, are more susceptible to weathering and erosion, as well as slope instability (**Figure 5b**).

3.2.6 Structural discontinuities

The association between structural discontinuity and rock slopes is a critical factor. The orientation of structural discontinuities was determined by collecting data facet-by-facet from the exposed rock mass and determining its affiliation to slope proclivities. Based on field observations and preliminary analysis joints and faults were considered the main geologic structures for further hazard/susceptibility/evaluations. Facet wise the structural data were collected and ratings were assigned based on the proposed slope susceptibility evaluation factors.

3.2.7 Rainfall manifestation

The average annual rainfall in the study area is 1372.8 mm. The amount of rain that falls has a significant impact on the slope's stability [25, 29, 43]. The instability of slopes increased as the amount and intensity of rainfall increased, which is obvious and reasonable. Due to the nature of the materials exposed in the slopes and the slopes' drainage characteristics, this is not always the case. As a result, rainfall-induced features are useful indicators for assessing the impact of rainfall on slope instabilities. Rainfall-induced slope manifestations (such as gully formation, toe erosion, and stream bank erosion) were taken into account when determining the rainfall rating (**Figure 7a**).

3.2.8 Human activity

Man-made activities, in addition to natural triggering parameters, increase the slopes' potential for instability [44]. Developmental activities such as road construction and cultivation activities are examples of man-made activities that affect slope stability conditions. Such anthropogenic activities increased the moisture content of soil or rock masses, as well as a reduction in slope stability (**Figure 7b**).

3.2.9 Landslide hazard zonation

For landslide hazard zonation, the slopes in the study area were divided into individual land facets. For this purpose, topographical map on 1:50,000 scales was utilized to delineate the land facets. A total of 106 slope land facets were delineated (**Figure 4**). Slope geometry includes relative relief and slope morphometry. From a total 110 km², 60.5 km² (55%) fall in to very high relative relief (>300 m), 24.2 km² (22%) fall in to high relative relief (201–300 m), 14.3 km² (13%) fall in to medium relative relief (101–200 m), and 11 km² (10%) fall in to moderate relative relief (51–100 m) (**Figure 6d**). Slope morphometry defines the steepness of the slopes. In the study area, about 18.87% of slopes fall under the category of escarpment/cliff (>45°) and 29.25% of slopes are a step (36–45°). The remaining slope falls under moderately steep slope (26–35°), gentle slope (16–25°), and very gentle slope (<15°) which account for 30.19, 15.09, and 6.60%, respectively (**Figure 6c**).

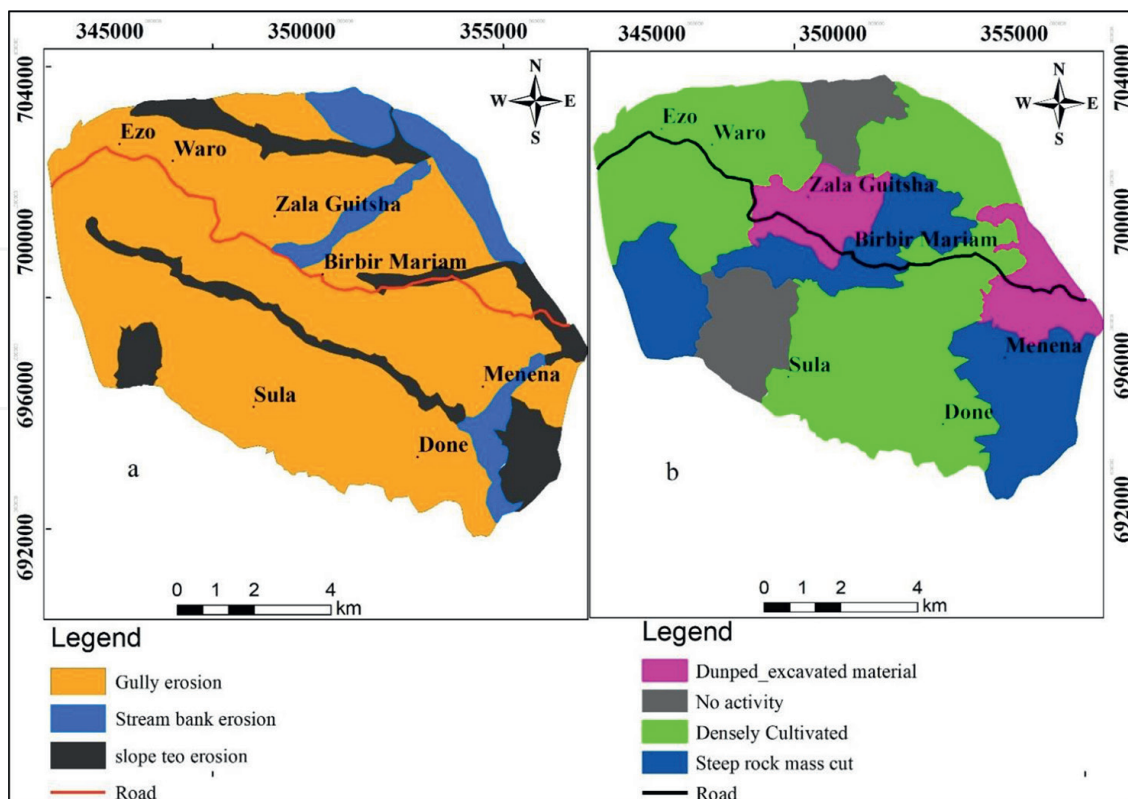


Figure 7.
a. Rainfall-induced surface manifestation map and b. anthropogenic developmental activities affecting slope stability.

The most dominant lithological units of the study area are highly disintegrated basalt. Spheroidal weathering was dominantly observed in the northwest and central parts of the study area (Figure 2). Faults, joints, and fractures are the dominant geological structures affecting the slope material. Residual soils and colluvial deposits are the most common slope materials (Figure 5b). Based on the map 58.11% of the total area is covered by soil mass, 28.3% is covered by disintegrated rock mass, and 18.87% is covered by medium-strong rock mass (Figure 5b).

Based on the land use-land cover, the major portion of the slopes is covered by agricultural land (43.4%). Moreover, areas covered by moderately vegetated, sparsely vegetated, and barren land account for 27.34, 18.87, and 10.39%, respectively. Surface indications such as damp, wet, dripping, and flowing water were considered for each facet to assess and evaluate the groundwater conditions. Watermarks, algal growth, and other features were also noted. As a result, each land facet was given a score (Figure 6a). A record of the rainfall in the study area shows that the months from April to June and from July to October received more rain. Rain-induced slope manifestations such as gully erosion, toe erosion, and stream bank erosion were also taken into account. Slope toe erosion, stream bank erosion, and gully erosion all accounted for 24.53, 20.75, and 54.72% of the total erosion (Figure 7a).

Manmade activities which affect the slope stability in the study area include cultivation activity, road construction, and unsafe dumping of materials. Based on field data-intensive cultivation activity covered about 43.4%, steep rock-cut for road construction constitute 26.4%, and unsafe dumped materials covered about 22.6%. About 7.6% of the total area falls under no human activities (Figure 7b). The study

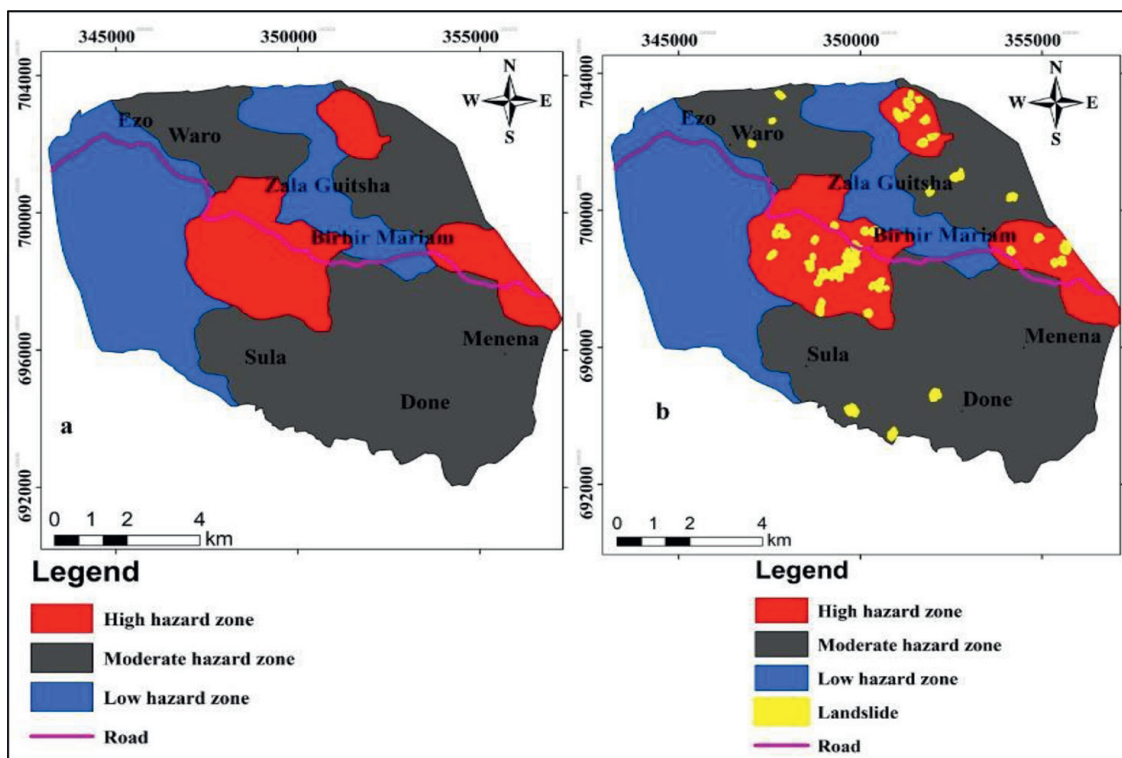


Figure 8.
 a. Landslide hazard zonation of Birbir Mariam and b. validation of present landslide hazard zonation map.

area's landslide hazard was determined facet-by-facet using an evaluated landslide hazard, which indicates the cumulative likelihood of instability. The area was divided into three zones based on the values of the assessed landslide hazard: high, moderate, and low hazard zones (**Figure 8a**).

4. Discussion

The selection and validity of the conditioning factors are of major importance for the correct result of the slope susceptibility evaluation parameter. Intrinsic and external causative parameter rating schemes were therefore considered to be responsible for slope instability. The high-hazard zones are mainly located in the central part and north-eastern side of the study area (**Figure 8a**). These localities are dominantly agricultural lands subjected to many anthropogenic activities. Most of the main road that crosses the area falls within the high-hazard zone areas. Along the main road, it is common to observe slope failures also in the form of earth slide rock falls (**Figure 8a**). Such failures mostly occurred following heavy rains. It was also reported that the main road experienced frequent failures and maintenance in the past. The problem still exists in the areas because of a lack of proper understanding of the causes and failure mechanisms of failures in the area. The southern and northeastern parts of the area fall under the moderate hazard zone, while the West and North West areas fall under the low hazard zone (**Figure 8a**). On the landslide hazard map of the study area, 18.87% (20.76 km²) is classified as high hazard, 54.72% (60.19 km²) is categorized as a moderate hazard, and 26.41% (29.05 km²) is divided into a low hazard (**Figure 8a**).

5. Validation of slope susceptibility evaluation rating scheme

By comparing the prepared landslide hazard zonation map of the current study area to existing landslide inventory data, the prepared landslide hazard zonation map was validated. The majority of the landslides occurred along the road and river banks. The landslide inventories were superimposed on the area's landslide hazard map. Based on the validation (by overlying), 37 (80.43%) of the 46 landslide inventory data fall into the high hazard zone, 9 (19.57%) into the moderate hazard zone, and none in the low hazard zone. As a result, the slope susceptibility rating scheme's landslide hazard zonation map is found to be reliable and comparable to real-world ground conditions (**Figure 8b**).

6. Conclusion

In highland and mountain terrain, landslide hazards and susceptibility zonation are critical for land use planning and development. A landslide hazard zonation map was produced using a slope susceptibility evaluation parameter rating scheme. The method takes into account both internal and external causative factors. The slope susceptibility evaluation parameter rating system is a feasible method of assigning numerical ratings to each site-specific intrinsic and external causative factor based on their role and contribution to slope instability. The Birbir Mariam area was subjected to the slope susceptibility evaluation parameter rating method. According to the results, there is a low hazard zone of 26.41% (29.05 km²), a moderate hazard zone of 54.72% (60.19 km²), and a high hazard zone of 18.87% (20.76 km²) in the study area. The generated landslide susceptibility zonation map was compared to actual past landslide activity data to ensure accuracy. According to the comparison, 37 (80.43%) of the 46 landslide inventory data fall into the high hazard zone, 9 (19.57%) into the moderate hazard zone, and none fall into the low hazard zone. As a result, the method used in this study, as well as the resulting landslide susceptibility zonation map, were found to be reliable and can be used in other areas with similar geologic and topographic conditions [45].

Acknowledgements

The authors are grateful to Arba Minch University for providing partial funds to conduct fieldwork and for allowing the first author to pursue his postgraduate studies. The Department of Geology of Arba Minch University is dually acknowledged for various administrative and technical supports during the research.

Conflict of interest

The authors report no potential conflicts of interest.

IntechOpen


IntechOpen

Author details

Yonas Oyda* and Hailu Regasa
Arba Minch University, Arba Minch, Ethiopia

*Address all correspondence to: yonasoyda777@gmail.com

IntechOpen

© 2022 The Author(s). Licensee IntechOpen. This chapter is distributed under the terms of the Creative Commons Attribution License (<http://creativecommons.org/licenses/by/3.0>), which permits unrestricted use, distribution, and reproduction in any medium, provided the original work is properly cited. 

References

- [1] Chi KH, Park NW, Lee K. Identification of Landslide area using remote sensing data and quantitative assessment of landslide hazard BT– Proceedings under IEEE International Symposium on Geoscience and Remote Sensing.
- [2] Ghosh S, Carranza EJM, Westen CJ, Jetten VG, Bhattacharya DN. Selecting and weighting of spatial predictors for empirical modeling of landslide susceptibility in Darjeeling Himalaya (India). *Geomorphology*. 2011;**131**. DOI: 10.1016/j.geomorph.2011.04.019
- [3] van Westen CJ, Castellanos E, Kuriakose SL. Spatial data for landslide susceptibility, hazard, and vulnerability assessment: An overview. *Engineering Geology*. 2008;**102**(3-4):112-131. DOI: 10.1016/j.enggeo.2008.03.010
- [4] Anbalagan R. Landslide hazard evaluation and zonation mapping in mountainous terrain. *Engineering Geology*. 1992;**32**(4):269-277. DOI: 10.1016/0013-7952(92)90053-2
- [5] Bernat Gazibara S, Krkač M, Mihalić Arbanas S. Landslide inventory mapping using LiDAR data in the City of Zagreb (Croatia). *Journal of Maps*. 2019;**15**(2):773-779. DOI: 10.1080/17445647.2019.1671906
- [6] Pham BT, Bui DT, Indra P, Dholakia MB. Landslide susceptibility assessment at a part of Uttarakhand Himalaya, India using GIS – Based statistical approach of frequency ratio method. *International Journal of Engineering Research And Technical Research*. 2015;**V4**(11):338-344. DOI: 10.17577/ijertv4is110285
- [7] Calligaris C, Poretti G, Tariq S, Melis MT. First Steps towards a Landslide Inventory Map of the Central Karakoram National Park. 72542017. DOI: 10.5721/EuJRS20134615
- [8] Erener A, Düzgün HSB. Landslide susceptibility assessment: What are the effects of mapping unit and mapping method? *Environmental Earth Sciences*. 2012;**66**(3):859-877. DOI: 10.1007/s12665-011-1297-0
- [9] Song Y, Niu R, Xu S, Ye R, Peng L, Guo T, et al. Landslide susceptibility mapping based on weighted gradient boosting decision tree in Wanzhou section of the three gorges reservoir area (China). *ISPRS International Journal of Geo-Information*. 2019;**8**(1). DOI: 10.3390/ijgi8010004
- [10] Lee S, Talib JA. Probabilistic landslide susceptibility and factor effect analysis. *Environmental Geology*. 2005;**47**. DOI: 10.1007/s00254-005-1228-z
- [11] Raghuvanshi TK, Ibrahim J, Ayalew D. Slope stability susceptibility evaluation parameter (SSEP) rating scheme - an approach for landslide hazard zonation. *Journal of African Earth Sciences*. 2014;**99**(PA2):595-612. DOI: 10.1016/j.jafrearsci.2014.05.004
- [12] Mulatu E, Raghuvanshi TK, Abebe B. Landslide hazard zonation around Gilgel gibe-II hydroelectric project, Southwestern Ethiopia. *SINET: Ethiopian Journal of Science*. 2011;**32**(1):9-20. DOI: 10.4314/sinet.v32i1.68733
- [13] Raghuvanshi TK, Negassa L, Kala PM. GIS based grid overlay method versus modeling approach - a comparative study for landslide hazard zonation (LHZ) in meta Robi District of west Showa zone in Ethiopia. *Egyptian*

Journal of Remote Sensing and Space Science. 2015;**18**(2):235-250.
DOI: 10.1016/j.ejrs.2015.08.001

[14] Seid JI, Raghuvanshi TK, Ayalew D. Landslide hazard zonation and slope instability assessment using optical and InSAR data: A case study from gidole town and its surrounding areas, Southern Ethiopia. *Hydrology & Meteorology*. 2014;**5**(4):7587

[15] Ayalew L, Yamagishi H. Slope failures in the Blue Nile basin, as seen from landscape evolution perspective. *Geomorphology*. 2004;**57**(1-2):95-116.
DOI: 10.1016/S0169-555X(03)00085-0

[16] Kanungo DP, Arora MK, Sarkar S, Gupta RP. Landslide susceptibility zonation (LSZ) mapping – A review. *Journal of South Asian Studies*. 2009;**2**

[17] Lee S, Pradhan B. Landslide hazard mapping at Selangor, Malaysia using frequency ratio and logistic regression models. *Landslides*. 2007;**4**. DOI: 10.1007/s10346-006-0047-y

[18] Dahal RK, Hasegawa S, Bhandary NP, Poudel PP, Nonomurac A, Yatabe Y. A replication of landslide hazard mapping at catchment scale. *Geomatics, Natural Hazards and Risk*. 2012

[19] Canoğlu MC. Deterministic landslide susceptibility assessment with the use of a new index (factor of safety index) under dynamic soil saturation: An example from demirciköy watershed (Sinop/Turkey). *Carpathian Journal of Earth and Environmental Sciences*. 2017;**12**(2):423-436

[20] Du G l, Zhang Y s, Iqbal J, Yang ZH, Yao X. Landslide susceptibility mapping using an integrated model of information value method and logistic regression in the Bailongjiang watershed, Gansu

Province, China. *Journal of Mountain Science*. 2017;**14**(2):249-268.
DOI: 10.1007/s11629-016-4126-9

[21] Silalahi FES, Pamela A, Y., & Hidayat, F. Landslide susceptibility assessment using frequency ratio model in Bogor, West Java, Indonesia. *Geoscience Letters*. 2019;**6**(1).
DOI: 10.1186/s40562-019-0140-4

[22] Ayalew L, Yamagishi H. The application of GIS-based logistic regression for landslide susceptibility mapping in the Kakuda–Yahiko Mountains, Central Japan. *Geomorphology*. 2005;**65**. DOI: 10.1016/j.geomorph.2004.06.010

[23] Guzzetti F, Reichenbach P, Ardizzone M, Cardinali M, Galli M. Estimating the quality of landslides susceptibility models. *Geomorphology*. 2006;**81**. DOI: 10.1016/j.geomorph.2006.04.007

[24] Meten M, Bhandary NP, Yatabe R. GIS-based frequency ratio and logistic regression modelling for landslide susceptibility mapping of Debre Sina area in Central Ethiopia. *Journal of Mountain Science*. 2015;**12**(6):1355-1372.
DOI: 10.1007/s11629-015-3464-3

[25] Woldearegay K. Review of the occurrences and influencing factors of landslides in the highlands of Ethiopia: With implications for infrastructural development. *Momona Ethiopian Journal of Science*. 2013;**5**(1):3. DOI: 10.4314/mejs.v5i1.85329

[26] Azeze AW. Modeling of Landslide Susceptibility in a Part of Abay Basin, Northwestern Ethiopia. March. 2020.
DOI: 10.1515/geo-2020-0206

[27] Chauhan S, Sharma M, Arora MK, Gupta NK. Landslide susceptibility zonation through ratings derived

from artificial neural network. *The International Journal of Applied Earth Observation and Geoinformation*. 2010;**12**. DOI: 10.1016/j.jag.2010.04.006

[28] Guzzetti F, Mondini AC, Cardinali M, Fiorucci F, Santangelo M, Chang KT. Landslide inventory maps: New tools for an old problem. *Earth-Science Reviews*. 2012;**112**(1-2):42-66. DOI: 10.1016/j.earscirev.2012.02.001

[29] Jeong S, Kassim A, Hong M, Saadatkhah N. Susceptibility assessments of landslides in Hulu Kelang area using a geographic information system-based prediction model. *Sustainability (Switzerland)*. 2018;**10**(8). DOI: 10.3390/su10082941

[30] Santangelo M, Gioia D, Cardinali M, Guzzetti F, Schiattarella M. Landslide inventory map of the upper Sinni River valley, southern Italy. *Journal of Maps*. 2015;**11**(3):444-453. DOI: 10.1080/17445647.2014.949313

[31] Kannan M, Saranathan E, Anbalagan R. Comparative analysis in GIS-based landslide hazard zonation—A case study in Bodi-Bodimettu Ghat section, Theni District, Tamil Nadu, India. *Arabian Journal of Geosciences*. 2015;**8**(2):691-699. DOI: 10.1007/s12517-013-1259-9

[32] Kundu S, Saha AK, Sharma DC, Pant CC. Remote sensing and GIS based landslide susceptibility assessment using binary logistic regression model: A case study in the Ganesh ganga watershed, Himalayas. *The Journal of the Indian Society of Remote Sensing*. 2013;**41**. DOI: 10.1007/s12524-012-0255-y

[33] Legorreta Paulín G, Bursik M, Hubp JL, Mejía LMP, Aceves Quesada F. A GIS method for landslide inventory and susceptibility mapping in the Río El Estado watershed, Pico de Orizaba

volcano, México. *Natural Hazards*. 2014;**71**(1):229-241. DOI: 10.1007/s11069-013-0911-8

[34] Mezughi TH, Akhir JM, Rafek AG, Abdullah I. Landslide susceptibility mapping using the statistical index method and factor effect analysis along the E- W highway (Gerik - Jeli), Malaysia. *Australian Journal of Basic and Applied Sciences*. 2011;**5**(6):847-857

[35] Sarkar S, Roy AK, Martha TR. Landslide susceptibility assessment using information value method in parts of the Darjeeling Himalayas. *Journal of the Geological Society of India*. 2013;**82**(4):351-362. DOI: 10.1007/s12594-013-0162-z

[36] Shahabi H, Hashim M. Landslide susceptibility mapping using GIS-based statistical models and remote sensing data in tropical environment. 2015. 1-15. DOI: 10.1038/srep09899

[37] Abbate E, Bruni P, Sagri M. *Geology of Ethiopia: A Review and Geomorphological Perspectives*. 2015. DOI: 10.1007/978-94-017-8026-1

[38] Bonini M, Corti G, Innocenti F, Manetti P, Mazzarini F, Abebe T, Pecskey Z. Evolution of the main Ethiopian rift in the frame of Afar and Kenya rifts propagation. February. 2005. DOI: 10.1029/2004TC001680

[39] Ebinger C, Yemane T, Woldegabriel G, Aronson J. Late Eocene-Recent volcanism and faulting in the Southern Main Ethiopian Rift. February. 1993. DOI: 10.1144/gsjgs.150.1.0099

[40] Philippon M, Corti G, National I, Sani F. Evolution, distribution and characteristics of rifting in Southern Ethiopia. April. 2014. DOI: 10.1002/2013TC003430

[41] Ermias B, Raghuvanshi TK, Abebe B. Landslide Hazard zonation (LHZ) around Alemketema town, north Showa zone, Central Ethiopia - a GIS based expert evaluation approach. *International Journal of Earth Sciences and Engineering*. 2017;**10**(01):33-44. DOI: 10.21276/ijee.2017.10.0106

[42] Lee S, Choi J, Min K. Landslide susceptibility analysis and verification using the Bayesian probability model. *Environmental Geology*. 2002;**43**. DOI: 10.1007/s00254-002-0616-x

[43] Ayalew L. The effect of seasonal rainfall on landslides in the highlands of Ethiopia. *Bulletin of Engineering Geology and the Environment*. 1999;**58**(1):9-19. DOI: 10.1007/s100640050065

[44] Kanungo DP, Arora MK, Sarkar S, Gupta RP. A fuzzy set based approach for integration of thematic maps for landslide susceptibility zonation. *Georisk*. 2009;**3**

[45] Das I, Stein A, Kerle N, Dadhwal. Landslide susceptibility mapping along road corridors in the Indian Himalayas using Bayesian logistic regression models. *Geomorphology*. 2012;**179**. DOI: 10.1016/j.geomorph.2012.08.004